

# Wavefront-sensor tomography for measuring spatial coherence

Jaroslav Rehacek, Zdenek Hradil<sup>a</sup>, Bohumil Stoklasa<sup>a</sup>, Libor Motka<sup>a</sup>  
and Luis L. Sánchez-Soto<sup>b</sup>

<sup>a</sup> Department of Optics, Palacky University, 17. listopadu 12, 77146 Olomouc, Czech Republic;

<sup>b</sup> Departamento de Óptica, Facultad de Física, Universidad Complutense, 28040 Madrid, Spain

## ABSTRACT

Wavefront sensing is an advanced technology that enables the precise determination of the phase of a light field, a critical information for many applications, such as noncontact metrology, adaptive optics, and vision correction. Here, we reinterpret the operation of wavefront sensors as a simultaneous unsharp measurement of position and momentum. Utilizing quantum tomography techniques we report an experimental characterization and 3D imaging of a multimode laser light.

**Keywords:** Wavefront sensing, coherence, tomography, parameter estimation, 3D imaging

## 1. INTRODUCTION

Wavefront sensing<sup>1</sup> is an advanced optical technology providing direct access to phase properties of measured optical fields. In this sense wavefront sensing constitutes an invaluable information source about many aspects of the observed objects which are inaccessible to standard intensity detection methods but which are essential in many phase-dependent applications, such as metrology, high-power laser systems, adaptive optics etc.

Despite recent successful utilization of wavefront sensors in coherent light processing their full potential has yet to be explored. Recognizable analogies between wavefront sensing and tomography methods previously developed for quantum information processing hint at introducing a conceptionally new approach to wave front sensing based on tomography capable of characterizing general multimode optical fields.<sup>2,3</sup> Direct access to additional degrees of freedom of light that are reflected in the coherence properties of the measured signal is interesting from the fundamental point of view but also opens a wide range of potential applications of wavefront sensing techniques in state-of-art applications dealing with partially coherent light, such as quantum information processing, digital holography and 3D imaging. This can be illustrated by a simple motivating example of beam propagation, where to predict the intensity at the output of a known optical system, the knowledge of the input intensity alone is not sufficient<sup>4</sup> and information about the second order coherence properties of the signal needs to be supplied.

## 2. WAVEFRONT SENSING

The principle of the Shack-Hartmann (SH) wavefront sensor is shown in Fig. 1. Local slopes of the incoming wavefront<sup>1</sup> in the plane of the microlens array (SH plane) determine the positions of the bright spots in the lens focal plane (CCD plane), from which partial information about the transversal momentum of the signal can be extracted. This is the standard way of operating wavefront sensors. Unfortunately, should the signal be only partially coherent, that is, multimode, a single well-defined wavefront would not exist — the signal would be a statistical mixture of possibly many distinct wavefronts/modes<sup>5</sup> — and the standard wavefront measurement would fail. To circumvent this problem we notice that a detection at a particular pixel implies that the photon/photons must have passed through the associated subaperture, which amounts to unsharp position measurement on the incoming beam. Hence we may conclude that SH measurements with finite apertures are pertinent examples of simultaneous unsharp position and momentum measurements<sup>6</sup> that are of fundamental importance in physics and quantum theory in particular. Such an interpretation of the registered intensity profile, see Fig. 1 for example, is a key ingredient of our considerations.

---

Further author information: (Send correspondence to Jaroslav Rehacek)

Jaroslav Rehacek: E-mail: rehacek(at)optics.upol.cz, Telephone: +420 58 5634257

Unconventional Imaging and Wavefront Sensing 2015, edited by Jean J. Dolne,  
Thomas J. Karr, Victor L. Gamiz, Proc. of SPIE Vol. 9617, 961703 · © 2015 SPIE  
CCC code: 0277-786X/15/\$18 · doi: 10.1117/12.2188040

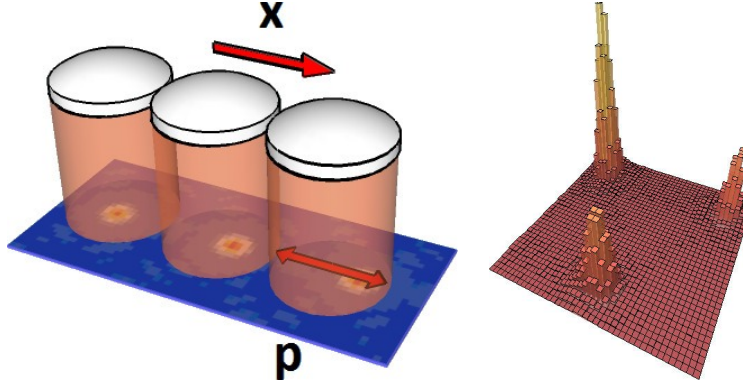


Figure 1. The measurement principle of SH detection and a typical intensity readout.

### 3. PARTIALLY COHERENT SIGNAL

Let us demonstrate that common wavefront sensors<sup>7</sup> can be utilized for measuring mutual coherence and hence 3D imaging of partially coherent fields provided quantum state reconstruction techniques are adopted for data processing. Taking advantage of the formal correspondence between wave optics and quantum mechanics we define  $\rho$  the coherence matrix describing the second-order coherence of measured signal  $G(x', x'') = \langle x' | \rho | x'' \rangle = \text{Tr}(\rho | x' \rangle \langle x'' |)$ , where the ket  $|x\rangle$  is a vector describing a point-like source located at  $x$  and  $\text{Tr}$  denotes matrix trace. In this sense, mutual coherence function is seen to be a position representation of the coherence matrix and intensity distribution across a transversal plane becomes  $I(x) = \text{Tr}(\rho | x \rangle \langle x |)$  and describes a position measurement realized *e.g.* by placing a point-like pixel of a CCD camera at the position  $x$  in the detection plane. Furthermore we can describe a coherent beam (mode), with a complex amplitude  $U(x)$ , by a ket  $|U\rangle$ , such that  $U(x) = \langle x | U \rangle$ .

Now consider the Shack-Hartmann measurement. Notation is simplified by setting the focal length of the microlenses and the effective wave number to unity, and describe 1D geometry of the measurement and detection only. This is equivalent to considering one row of microlenses and one row of CCD pixels only. Generalization to 2D geometry is obvious. Upon illuminating the microlens array (SH plane) by a coherent signal  $U(x)$ , assuming that the axis of  $i$ th microlens (lens) is displaced from the SH optical axis by  $\Delta x_i$ , this lens feels the displaced field  $U(x - \Delta x_i) = \langle x | \exp(-i\Delta x_i \hat{p}) | U \rangle$ . This field gets filtered and truncated by the lens aperture function  $A(x) = \langle x | A \rangle$  and Fourier transformed by the lens prior to being detected the SH focal plane (CCD plane),

$$\begin{aligned} U'(\Delta p_j) &= \int \langle A | x \rangle \langle x | e^{-i\Delta x_i \hat{p}} | U \rangle e^{-i\Delta p_i x} dx \\ &= \int \langle A | x \rangle \langle x | e^{-i\Delta p_i \hat{x}} e^{-i\Delta x_i \hat{p}} | U \rangle dx \\ &= \langle A | e^{-i\Delta p_i \hat{x}} e^{-i\Delta x_i \hat{p}} | U \rangle, \end{aligned} \quad (1)$$

where the closure relation is used in the last step, and we assume that the  $j$ th pixel is displaced from the SH optical axis by  $\Delta p_j$ . Adding together the intensity contributions of all the orthogonal modes comprising the signal coherence matrix, we find that the intensity measured at the  $j$ th pixel behind the  $i$ th lens is governed by a Born-like rule

$$I(\Delta x_j, \Delta p_j) = \text{Tr}(\rho |\pi_{ij}\rangle \langle \pi_{ij}|), \quad |\pi_{ij}\rangle = e^{i\Delta x_i \hat{p}} e^{i\Delta p_i \hat{x}} |A\rangle, \quad (2)$$

and consequently, each pixel of the SH device makes projection of the input signal on the position and momentum translated aperture state. Some interesting special cases of those aperture states are worth mentioning:

- Small lenses.  $A(x) \rightarrow \delta(x)$ ,  $|A\rangle \rightarrow |x=0\rangle$  implies  $|\pi_{ij}\rangle \rightarrow |x=\Delta x_i\rangle$  — a position eigenstate.
- Large lenses.  $A(x) \rightarrow 1$ ,  $|A\rangle \rightarrow |p=0\rangle$  implies  $|\pi_{ij}\rangle \rightarrow |p=\Delta p_j\rangle$  — a momentum eigenstate.
- Gaussian profile.  $A(x) = \exp(-x^2/2)$ ,  $|A\rangle = |\alpha=0\rangle$  implies  $|\pi_{ij}\rangle \rightarrow D(\alpha_{ij})|0\rangle = |\alpha_{ij}\rangle$  — a coherent-like Gaussian state of amplitude  $\alpha = \Delta x_i + i\Delta p_j$ .

Point-like lenses produce broad diffraction patterns in the CCD plane and information about the transversal momentum in the SH plane is lost. Conversely, very large apertures provide sharp momentum measurement with the corresponding loss of positional sensitivity. The last case is the most interesting one: SH devices with Gaussian-apodized microlenses are capable of projecting the signal on a set of coherent states and hence yield direct sampling of Husimi quasiprobability distribution  $Q(\alpha) = \langle \alpha | \rho | \alpha \rangle$ . This provides a convenient phase space description of the signal: Different choices of CCD pixels and/or microlenses can be interpreted as particular translations in that phase space in a very close analogy to translations induced by changing the amplitude of the local oscillator in unbalanced homodyne tomography. The well known correspondence between the signal phase space description and the signal state itself demonstrates informational completeness of such an SH measurement.

#### 4. REALISTIC PICTURE

Experimental demonstration of SH tomography principles faces an obstacle that needs to be considered. The apertures of microlenses comprising a real wavefront sensor do not overlap and unlike the Gaussian profiles discussed above are spatially bounded structures. Introducing notation  $\Pi_{ij} = |\pi_{ij}\rangle\langle\pi_{ij}|$ , the measurement operators describing two pixels belonging to distinct apertures are found to be compatible  $[\Pi_{ij}, \Pi_{i'j}] = 0$ ,  $i \neq i'$ , which renders the tomography scheme informationally incomplete. Signal components passing through distinct apertures are never recombined and the mutual coherence of those components thus cannot be determined. The remedy here is to exclude all spatially bounded modes from the search space.<sup>8,9</sup> Indeed, spatially bounded modes carry infinite energy and for this reason are unphysical and impossible to generate with finite resources. Such truncation can be done by decomposing the signal in a suitable discrete spatially-unbounded computational basis realizable by sets of plane waves, Gaussian beams, Laguerre-Gaussian beams, etc. depending on the actual experimental context.

We denote the basis states  $|k\rangle$ ,  $k = 1, \dots, d$ , assuming orthonormality  $\langle k | l \rangle = \delta_{kl}$ ,  $k \neq k'$ , their complex amplitudes being  $\langle x | k \rangle = \psi_k(x)$ . With this notation the signal coherence matrix  $\rho$  and the measurement operators  $\Pi_{ij}$  live in  $d$ -dimensional Hilbert space and are parameterized as  $d \times d$  non-negative matrices. In order to reconstruct  $d^2$  real parameters of  $\rho$  we need to have  $d^2$  linearly independent measurements. Convenient matrix representation of measurement  $\Pi_{ij}$  in terms of complex amplitudes can be obtained directly from Eq. (2),

$$(\Pi_{ij})_{kl} = \psi_{l,i}(\Delta p_j) \psi_{k,i}^*(\Delta p_j), \quad (3)$$

where  $\psi_{k,i}(x)$  is the complex amplitude in the CCD plane of the  $i$ -th lens generated by the incident  $k$ -th basis mode  $\psi_k$ .

Let us illustrate the idea with a conceptually simple and practically important example of an SH sensor with square lenses  $|A\rangle = \int_{-1/2}^{1/2} |x\rangle dx$  and  $A(x) = \text{rect}(x)$ . The signal will be decomposed in a discrete basis set of plane waves parametrized by transverse momenta  $p_k$ :  $|k\rangle = |p_k\rangle$ ,  $\psi_k(x) = \exp(-ip_k x)$ . This is Fraunhofer diffraction on a slit so the measurement matrix is immediately obtained in the form

$$(\Pi_{ij})_{kl} = \text{sinc}(\Delta p_j + p_k) \text{sinc}(\Delta p_j + p_l) e^{i(p_l - p_k) \Delta x_i}. \quad (4)$$

Wavefront detection with a single square lens can never be informationally complete. Let us analyze the smallest possible search space consisting of just two plane waves, which is equivalent to a single-qubit tomography. By considering different pixels  $j$  all belonging to the same aperture  $i$ , linear combinations of only three out of the total of four Pauli matrices can be generated from Eq. (4). For example, a lens placed on the SH axis having  $\Delta x_i = 0$  fails to generate  $\sigma_y$  matrix and at least one more lens with a different displacement  $\Delta x_i$  needs to be added to the setup to make the tomography complete. This argument can be extended to larger dimensions: The larger search space, the more microlenses must be used to characterize the signal completely.

#### 5. MULTIMODE LASER BEAM PROPAGATION

In the proposed experiment, a genuinely multi-mode light of a Nd:YAG pulsed laser operating in the deep ultraviolet region served as an example of partially coherent signal. Since laser light can be advantageously decomposed into the Hermite-Gaussian (HG) superposition, these were used as a basis for the coherence function

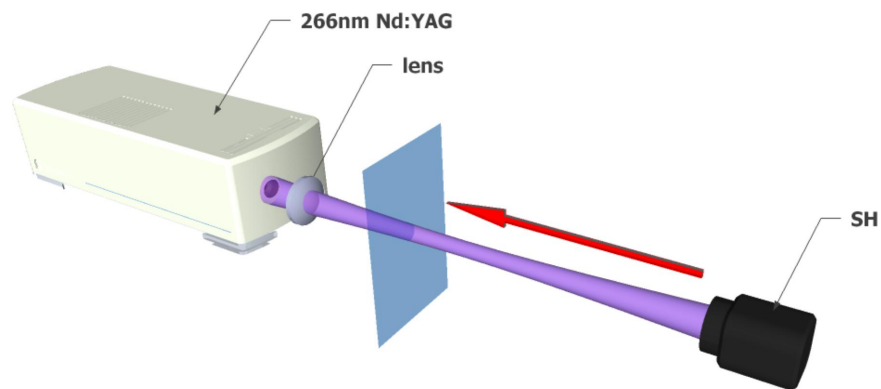


Figure 2. Experimental setup. A multi-mode Nd:YAG laser beam is detected with an SH sensor and characterized in the SH plane with the help of the SH tomography.<sup>6</sup> The calculated coherence matrix is numerically propagated back to the blue plane, where the inferred transverse beam intensity profile is compared to the actual CCD scan.

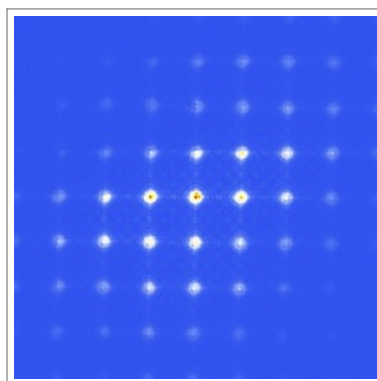


Figure 3. Typical experimental SH data. About six thousand pixels are analyzed with our SH tomography technique to characterize the coherence matrix of the detected Nd:YAG laser beam.

representation. Reconstructed space was restricted to 9 active modes, that is, 81 entries of the coherence matrix had to be estimated. At least 81 independent measurements are required to accomplish this task. In our experiment, much larger data sets composed of intensity data from  $11 \times 11$  pixels for  $7 \times 7$  array of microlenses, i.e. 5929 measurements in total, was used for the SH tomography to suppress reconstruction artifacts.

Shack-Hartmann sensor was realized in Meopta-Optika with  $150\mu\text{m}$  microlens pitch,  $4.6\mu\text{m}$  CCD pixel size and  $7\text{mm}$  microlens to CCD distance. The waist size of the basic HG mode is a prior parameter of the reconstruction and was estimated to  $0.3\text{mm}$ .

The reconstructed coherence matrix shown in Fig. 4 clearly shows partially coherent nature of the Nd:YAG beam. Non-zero diagonal elements indicate many active modes in the beam, while non-zero off-diagonal elements describe existing correlations between the modes. Due to possibility to express any partially coherent field as a superposition of coherent modes, singular value decomposition of the coherence matrix can be used to reconstruct these modes along with their amplitude and phase profiles.

To validate the reconstruction, a free space (back)propagation of the laser beam around the beam waist was performed, see Fig. 4. The coherence matrix was measured in a plane  $250\text{mm}$  behind the waist, where an intensity profile was reconstructed and compared to a direct intensity scan measured by a CCD camera. Then, the reconstructed coherence matrix was digitally transported back to the plane located on the opposite side of the waist  $220\text{mm}$  distant from the waist. Again, beam intensity profile was calculated from the coherence matrix and compared to a direct intensity measurement. Correlation coefficients between the reconstructed and

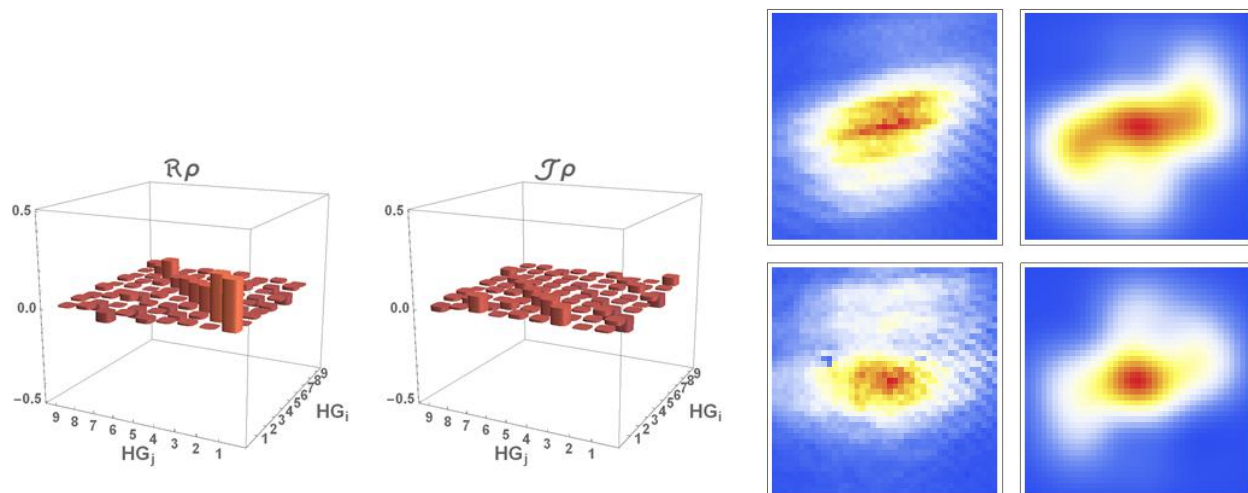


Figure 4. Nd:YAG laser beam propagation. Left panel: a reconstructed coherence matrix  $\rho$  of the beam in the Hermite-Gaussian (HG) basis, real and imaginary parts are plotted separately. Indexes  $i, j$  label HG modes in the following order:  $HG_{0,0}$ ,  $HG_{1,0}$ ,  $HG_{2,0}$ ,  $HG_{0,1}$ ,  $HG_{1,1}$ ,  $HG_{2,1}$ ,  $HG_{0,2}$ ,  $HG_{1,2}$ ,  $HG_{2,2}$ . Right panel: comparison of numerical simulation of intensity propagation and directly measured intensity distributions. The top row contains data of initial plane, when left is a direct CCD scan and right intensity reconstruction from the coherence matrix. The bottom row contains data from a plane 550mm away of the initial plane. Left is a direct CCD scan and right intensity reconstruction from propagated coherence matrix.

measured intensity profiles are 0.93 for the input plane and 0.91 for the output plane. Since free space intensity propagation requires detailed knowledge of the beam coherence properties, high correlation coefficients witness successful SH tomography.

## 6. CONCLUSIONS

We experimentally demonstrated feasibility of the new Shack-Hartmann tomography for intensity propagation of multimode light by measuring Nd:YAG laser beam. Using the representation of Hermite-Gaussian modes, we observed nontrivial spatial correlations in the beam which provide us all information needed for successful intensity propagation. The numerical prediction of the beam propagation was compared with direct intensity measurements to prove the correctness of the reconstruction. As the method is a single-shot measurement and the Shack-Hartmann sensor is easy to build cost effective device, there is a great potential for implementing this technique in general 3-D imaging problems.

## ACKNOWLEDGMENTS

This work is co-financed by the European Social Fund and the state budget of the Czech Republic, project No. CZ.1.07/2.3.00/30.0041 (POST-UP II), and supported by the Grant Agency of the Czech Republic, Grant No. 15-031945.

## REFERENCES

- [1] Platt, B. C. and Shack, R. S., "History and principles of Shack-Hartmann wavefront sensing," J. Refract. Surg. 17, S573-S577 (2001).
- [2] Hradil, Z., Rehacek, J. and Sánchez-Soto, L. L., "Quantum Reconstruction of the Mutual Coherence Function," Phys. Rev. Lett. 105, 010401 (2010).
- [3] Waller, L., Situ, G. and Fleischer, J. W., "Phase-space measurement and coherence synthesis of optical beams," Nature Photonics 6, 474 (2012).
- [4] Goodman, J. W., [Introduction to Fourier Optics], Roberts Publishers, Colorado (2005).

- [5] Goodman, J. W., [Statistical Optics], Wiley-Interscience, New York (2000).
- [6] Stoklasa, B., Motka, L., Rehacek, J., Hradil, Z. and Sánchez-Soto, L. L., “Wavefront sensing reveals optical coherence,” *Nat. Commun.* 5, 10.1038 (2014).
- [7] Geary, J. M., [Introduction to Wavefront Sensors], SPIE-International Society for Optical Engineering, Bellingham, WA (1995).
- [8] Hradil Z., Mogilevtsev, D. and Rehacek, J., “Biased tomography schemes: An objective approach,” *Phys. Rev. Lett.* 96, 230401 (2006).
- [9] Rehacek, J., Hradil, Z., Bouchal, Z., Celechovsky, R., Rigas, I. and Sánchez-Soto, L. L., “Full Tomography from Compatible Measurements,” *Phys. Rev. Lett.* 103, 250402 (2009).